IJST, Transactions of Mechanical Engineering, Vol. 38, No. M1+, pp 167-179
Printed in The Islamic Republic of Iran, 2014

A POINTWISE APPROACH FOR ENFORCEMENT OF ESSENTIAL BOUNDARY CONDITIONS IN THE ISOGEOMETRIC ANALYSIS*

Y. BAZARGAN-LARI**

Dept. of Mechanical Eng., Shiraz Branch, Islamic Azad University, Shiraz, I. R. of Iran
Email: bazarganlari@iaushiraz.ac.ir

Abstract– Isogeometric analysis is a recently developed numerical technique that uses NURBS basis functions instead of Lagrange polynomial basis functions used in standard finite element method. This allows the analysis to be done with the exact CAD geometry that it is based on. However, the non interpolatory property of NURBS basis functions makes the essential boundary condition imposition to be no longer applicable, directly on the control values. Therefore, a technique such as penalty method or fitting of the boundary data onto the span of the basis functions is needed. Such techniques usually lead to additional computational complexity or cost. In the present paper, a simple pointwise approach is proposed to accurately impose essential boundary conditions in the isogeometric analysis. The method is based on the collocation of boundary conditions in distinct points on the boundary using NURBS basis functions. Some numerical examples in heat conduction and linear elasticity are used to evaluate applicability and accuracy of the proposed method. It is shown, through demonstrative numerical examples, that the present method can improve the accuracy of the isogeometric analysis.

Keywords– Isogeometric analysis, essential boundary conditions, NURBS basis functions, potential problems, linear elasticity

1. INTRODUCTION

Today, many problems in the vast fields of science and engineering are routinely solved using the finite element (FE) method. To perform an analysis using this method, it is necessary to generate a mesh describing the geometry of the problem to be analyzed. To do this, a computer aided design (CAD) system is commonly employed to extract geometric data which is used in the mesh generation process. Each of these disciplines has evolved independently and recent research efforts have been directed to unify these two areas. Isogeometric analysis (IA), proposed by Hughes and his colleagues, is a new numerical simulation approach that combines the FE method and CAD technology into a unified framework. The FE meshes are replaced by parametric surfaces or volumes and the isoparametric concept is employed with the variational formulation. Some notable advantages are [1]: the exact and unified geometric representation, easy constructed high order continuous element and a superior accuracy compared with classic FE method. Due to its advantages, the IA rapidly widened its applications in many fields such as structural vibrations [2], fluid structure interactions [3], sensitivity analyses [4], turbulent flow simulations [5], shell analyses [6] and many others.

Unfortunately, the NURBS basis functions, as with many meshless methods, are not interpolatory at control points and the essential boundary conditions cannot be directly applied onto the control values [7].

*Received by the editors February 2, 2013; Accepted March 5, 2014.

Some efforts have been made so far to overcome this difficulty. A weak method of enforcement has been presented by Bazilevs & Hughes for the fluid mechanics problems [8, 9]. This approach requires additional terms in the weak form of the boundary value problem and may not provide sufficient accuracy in many problems. Least square is another technique for the enforcement of boundary conditions [1, 10, 11]. This method requires the solution of a potentially large set of matrix equations along the boundary, leading to additional computational costs. Penalty function method, a simple and well-known approach for imposition of boundary conditions, is also used in the IA [12]. The accuracy of this method depends on the penalty coefficient which must be determined by trial and error. The Nitsche method, first proposed in the 70s, is an attractive method which has been successfully used in meshless methods. The approach has also been applied on the IA [13]. The other method which is proposed to overcome this situation is based on a transformation method to modify the basis functions of the IA in order to impose boundary conditions [14].

The contribution of the current work is to introduce a simple pointwise approach for the imposition of essential boundary conditions in the IA. In this method, the exact value of the boundary condition is collocated on the distinct boundary points and the resulting equations are inserted into the system of equations. To evaluate the applicability of the proposed method, two model equations, heat conduction and linear elasticity, over 2D domains are selected and some numerical examples are solved for different grid sizes. The results are then compared with exact or finite element solutions and the convergence and accuracy of the proposed method are examined. It is observed that the present method can improve the accuracy of the IA.

2. MODEL BOUNDARY VALUE PROBLEMS

Our main goal in the current work is to develop a simple method for imposition of essential boundary conditions in the NURBS based IA. Therefore, without loss of generality, two model boundary value problems are considered to evaluate the proposed method. The first model problem is heat equation and the second one is elastostatic problem which are defined on two dimensional domain Ω with boundary $\partial\Omega$. The heat equation and its boundary conditions are as follows:

$$\begin{cases} \nabla^2 u + S = 0 & \text{in} \quad \Omega \\ \nabla u \cdot \boldsymbol{n} = \bar{t} & \text{on} \quad \Gamma^N \\ u = \bar{u} & \text{on} \quad \Gamma^E \end{cases} \tag{1}$$

where scalar u is the field variable, S is the source function, Γ^N and Γ^E denote the natural and essential boundaries, respectively. $\boldsymbol{n}$ is the unit outward normal vector to the boundary. $\bar{t}$ and $\bar{u}$ are prescribed flux and field variable on the boundary, respectively.

The governing equation and boundary conditions of the second model problem, linear elastostatic, are as follows:

$$\begin{cases} \boldsymbol{\nabla} \cdot \boldsymbol{\sigma} + \boldsymbol{b} = 0 & \text{in} \quad \Omega \\ \boldsymbol{\sigma n} = \bar{\boldsymbol{t}} & \text{on} \quad \Gamma^N \\ \boldsymbol{u} = \bar{\boldsymbol{u}} & \text{on} \quad \Gamma^E \end{cases} \tag{2}$$

where $\boldsymbol{u}$ is displacement vector, $\boldsymbol{\sigma}$ is stress tensor, $\boldsymbol{b}$ is body force vector, Γ^N and Γ^E denote the natural and essential boundaries, respectively. $\boldsymbol{n}$ is unit outward normal vector to the boundary. $\bar{\boldsymbol{t}}$ and $\bar{\boldsymbol{u}}$ are prescribed traction and displacements on the boundary, respectively. A schematic representation of problem domain and its boundaries, for both model equations, is shown in Fig. 1.

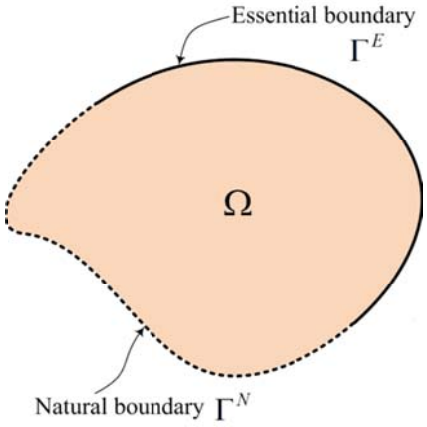

Fig. 1. A schematic representation of problem domain and its boundaries

3. NURBS BASIS FUNCTIONS

The aim of this section is to present a quick glance over NURBS and to introduce an overview of the IA. The NURBS basis functions are formed from linear combinations of B-spline basis functions [15]. Consider parametric space $\xi \in [0,1]$ in one dimension, to formulate a set of n B-spline basis functions of order p, a knot vector $\boldsymbol{\kappa}_\xi$ is defined as:

$$\boldsymbol{\kappa}_\xi = [\xi_1, \xi_2, \dots, \xi_{n+p+1}]^T \tag{3}$$

The knot vector $\boldsymbol{\kappa}_\xi$ is said to be open if the end knots are repeated $p+1$ times. With the given knot vector $\boldsymbol{\kappa}_\xi$, the univariate B-spline basis function N_{ap} can be constructed by the following recursive formula:

$$N_{a0}(\xi) = \begin{cases} 1, & \xi_a \le \xi < \xi_{a+1} \\ 0, & \text{otherwise} \end{cases} \qquad \text{for} \quad p = 0 \tag{4}$$

and

$$N_{ap}(\xi) = \frac{\xi - \xi_a}{\xi_{a+p} - \xi_a} N_{a(p-1)} + \frac{\xi_{a+p+1} - \xi}{\xi_{a+p+1} - \xi_{a+1}} N_{(a+1)(p-1)} \quad \text{for} \quad p \ge 1 \tag{5}$$

It is noted that the B-spline basis functions generally can be C^1 continuous and have non-interpolatory nature in the interior domain, while the basis functions defined by the open knot vector do interpolate at both end points.

If every B-spline function N_{ap} is set to have a weight w_a, a weighted form of the B-spline function, the so called NURBS basis function, R_a^p, can be defined as:

$$R_a^p(\xi) = \frac{N_{ap}(\xi) w_a}{\sum_{b=1}^{n} N_{bp}(\xi) w_b} \tag{6}$$

By using the NURBS basis functions, a curve $\boldsymbol{C}(\xi)$ can be constructed as:

$$\boldsymbol{C}(\xi) = \sum_{a=1}^{n} R_a^p(\xi) \boldsymbol{P}_a \tag{7}$$

where, $\boldsymbol{P}_a$ denotes the control point coordinate.

The two dimensional NURBS basis functions can be constructed by taking the tensor product of two one dimensional basis functions:

$$R_{ab}^{pq}(\boldsymbol{\xi}) = \frac{N_{ap}(\xi) N_{bq}(\eta) w_{ab}}{\sum_{c=1}^{n} \sum_{d=1}^{m} N_{cp}(\xi) N_{dq}(\eta) w_{cd}} \tag{8}$$

where, $\boldsymbol{\xi}$ is defined as (ξ, η) and w_{ab} represents the geometry related weight. The basis functions $N_{ap}(\xi)$ are defined in Eqs. (4) and (5). $N_{bq}(\eta)$ is the basis function of order q in the η dimension, which also follows from Eqs. (4) and (5) with the knot vector $\boldsymbol{\kappa}_\eta$ given by:

$$\boldsymbol{\kappa}_{\eta} = [\eta_1, \eta_2, \dots, \eta_{m+q+1}]^T \tag{9}$$

with m being the number of basis functions that comprise the B-spline in η direction. Similar to the curve representation of Eq. (7), a two dimensional surface $\boldsymbol{S}$ can be formulated as:

$$\boldsymbol{S} = \sum_{a=1}^{n} \sum_{b=1}^{m} R_{ab}^{pq}(\boldsymbol{\xi}) \boldsymbol{P}_{ab} \tag{10}$$

where, $\boldsymbol{P}_{ab}$ refers to the coordinate of the control points in the physical space. In other words, the Eq. (10) represents a mapping that maps any point from the parametric domain (ξ, η) to the physical domain (x, y).

4. ISOGEOMETRIC ANALYSIS

In Eq. (10) the NURBS basis functions are used for representation of a bivariate function. This notion can then be extended to the geometry representation of the problem domain and also the field variable approximation. In other words, in the NURBS based IA, field variable vector $\boldsymbol{u}$ and also the domain geometry are represented similarly to the isoparametric finite element method as follows:

$$\boldsymbol{u} \simeq \boldsymbol{u}^h = \sum_{A=1}^{NCP} R_A(\boldsymbol{\xi}) \boldsymbol{u}_A = \boldsymbol{R}^T \boldsymbol{U} \tag{11}$$

$$\boldsymbol{x} = \sum_{A=1}^{NCP} R_A(\boldsymbol{\xi}) \boldsymbol{P}_A = \boldsymbol{R}^T \boldsymbol{P} \tag{12}$$

where, NCP represents the total number of control points as well as the total number of basis functions. For convenience, the control points are re-numbered with a unified subscript "A" based on the subscripts {a, b} in Eq. (8) and the superscripts of basis function are ignored. Based on this, $R_A(\boldsymbol{\xi})$ is the NURBS basis function as defined in Eq. (8). $\boldsymbol{u}_A$ and $\boldsymbol{P}_A$ are the control variable and the position vector of the control point A, respectively. In a similar manner, $\boldsymbol{U}$ and $\boldsymbol{P}$ are the global control variable vector and the global position vector, respectively. $\boldsymbol{R}$ also is a matrix of basis functions. In other words, Eq. (12) maps any point $\boldsymbol{\xi}$ from the parametric space to a point $\boldsymbol{x}$ in the physical space.

By converting the model differential equations and natural boundary conditions given in Eq. (1) or in Eq. (2) to the integral weak form, then introducing the field variable approximation given in Eq. (11) and using the Galerkin method, the discrete form of the model equations can be obtained as follows [16].

$$\boldsymbol{K}\boldsymbol{U} = \boldsymbol{L} \tag{13}$$

where $\boldsymbol{K}$ is the coefficient matrix (stiffness matrix), $\boldsymbol{U}$ is the vector of unknown control values and $\boldsymbol{L}$ is the loading vector due to source function and natural boundary conditions. For the first model problem, the heat equation, coefficient matrix $\boldsymbol{K}$ and load vector $\boldsymbol{L}$ can be obtained as follows [16].

$$(\boldsymbol{K})_{AB} = \int_{\Omega} \left(\frac{\partial R_A}{\partial x} \frac{\partial R_B}{\partial x} + \frac{\partial R_A}{\partial y} \frac{\partial R_b}{\partial y} \right) d\Omega \quad , \quad (\boldsymbol{L})_A = \int_{\Omega} R_A S d\Omega + \int_{\Gamma^N} R_A \bar{t} d\Gamma \tag{14}$$

In a concise form, $\boldsymbol{K}$ and $\boldsymbol{L}$ can be obtained for the second model problem, elastostatic equation, as follows [16].

$$\boldsymbol{K} = \int_{\Omega} (\boldsymbol{B}\boldsymbol{R})^T \boldsymbol{D} (\boldsymbol{B}\boldsymbol{R}) d\Omega \quad , \quad \boldsymbol{L} = \int_{\Omega} \boldsymbol{R}^T \boldsymbol{b} d\Omega + \int_{\Gamma^N} \boldsymbol{R}^T \bar{\boldsymbol{t}} d\Gamma \tag{15}$$

where $\boldsymbol{B}$ is the strain differential operator and $\boldsymbol{D}$ is the elasticity matrix which are explained in detail in [16].

The elements in NURBS based IA are defined by the knot spans. Therefore, the domain integrals in Eqs. (14) and (15) can be evaluated using the traditional Gauss quadrature integration formula over these elements.

Similar to the majority meshfree methods, the NURBS basis functions don't generally fulfill the Kronecker delta property. The non-interpolatory property of the basis functions makes the control points not located within the physical domain. The most immediate result of the non-interpolatory property of NURBS basis functions is that it is not trivial to impose essential boundary into the control points.

Therefore, special techniques are needed to satisfy these boundary conditions. A brief summary on these methods was presented in the introduction.

5. TREATMENT OF ESSENTIAL BOUNDARY CONDITIONS

In this section, a simple point collocation approach is proposed to enforce exact boundary conditions in distinct points on the boundary. To explain this, assume $\boldsymbol{x}_0$ as a collocation point on the essential boundary in the physical space. The exact value of boundary condition in this point can be obtained from Eq. (1 or 2) as $\bar{u}(\boldsymbol{x}_0)$. On the other hand, the corresponding coordinate of point $\boldsymbol{x}_0$ on the parametric space, which is here denoted by $\boldsymbol{\xi}_0$, can be obtained via an inverse transformation using Eq. (12). Now, the field variable approximation function given in Eq. (11) can be invoked to derive a collocation equation for this boundary point as follows:

$$\bar{u}(\boldsymbol{x}_0) = \sum_{A=1}^{NCP} R_A(\boldsymbol{\xi}_0) u_A \tag{16}$$

In other words, the foregoing equation guarantees the exact satisfaction of boundary condition in the collocation point $\boldsymbol{x}_0$. Eq. (16) can be rewritten as follows:

$$[R_1(\boldsymbol{\xi}_0), R_2(\boldsymbol{\xi}_0), \dots, R_{NCP}(\boldsymbol{\xi}_0)]\boldsymbol{U} = \bar{u}(\boldsymbol{x}_0) \tag{17}$$

The last thing is to insert Eq. (17) into the system of equations given in Eq. (13). To do so, as proposed in the present work, we first find the nearest boundary control point to the collocation point $\boldsymbol{x}_0$ and then replace the associated equation in Eq. (13) with Eq. (17). A schematic representation of collocation point $\boldsymbol{x}_0$ and its nearest control point is shown in Fig. 2. Finally, the following algorithm summarizes the proposed procedure of imposition of essential boundary conditions.

a- Get the collocation point $\boldsymbol{x}_0$ and corresponding boundary condition $\bar{u}(\boldsymbol{x}_0)$.
b- Compute the parametric coordinate $\boldsymbol{\xi}_0$ using inverse transformation of Eq. (12).
c- Generate the point collocation equation given in Eq. (17).
d- Find the nearest control point to the point $\boldsymbol{x}_0$ and denote it by A_0.
e- In the system of equations given in Eq. (13) replace the associated equation of control point A_0 with Eq. (17).

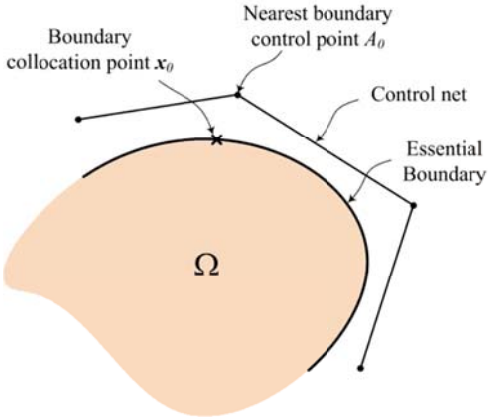

Fig. 2. A schematic representation of boundary collocation point and its nearest boundary control point

6. NUMERICAL EXAMPLES

To evaluate the applicability of the proposed method, two numerical examples are solved for each model's set of equation and boundary conditions in Eqs. (1 and 2) and the results are compared with the analytic or finite element solutions. The numerical integration within each element is carried out by 4×4 Gauss quadrature formula. In the numerical results presented here, the legend "direct" implies that the essential

boundary conditions are directly applied on the control variables and "present" denotes that the present approach is employed for boundary condition enforcement. All the error measures are computed based on the L_2 error norm of the field variables. In the first model equation, the error norm is obtained using the following formula

$$e = \frac{\int_\Omega \left(u^h - u^e\right)^2 d\Omega}{\int_\Omega (u^e)^2 d\Omega} \tag{18}$$

where, u^h is the numeric solution obtained from the proposed method and u^e is the exact solution. In the second model equation, a similar formula is used as follows

$$e = \frac{\int_\Omega \left(\boldsymbol{u}^h - \boldsymbol{u}^e\right)^{\mathrm{T}} \left(\boldsymbol{u}^h - \boldsymbol{u}^e\right) d\Omega}{\int_\Omega (\boldsymbol{u}^e)^{\mathrm{T}} (\boldsymbol{u}^e) d\Omega} \tag{19}$$

where, $\boldsymbol{u}^h$ is the displacement vector obtained from the proposed method and $\boldsymbol{u}^e$ is the exact displacement.

Example 1: Heat conduction in a unit square

As the first example, the potential problem given in Eq. (1) with the following source function is defined here in a unit square.

$$S = 2\pi^2 \sin(\pi x) \cos(\pi y) \tag{20}$$

The problem domain is shown in Fig. 3 and the exact solution for this problem is given as:

$$u = \sin(\pi x) \cos(\pi y) \tag{21}$$

This problem is subjected to essential boundary conditions generated according to the exact solution of Eq. (21) on all four sides of the problem domain.

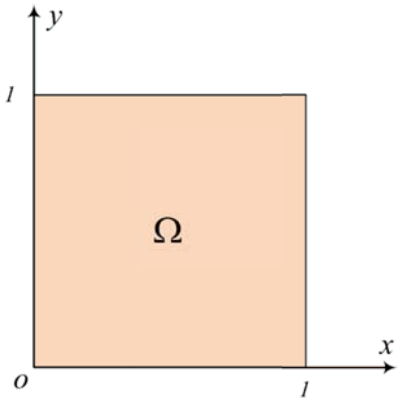

Fig. 3. Unit square, example 1

To evaluate the convergence of the proposed method, the problem is solved using 11 control nets with different resolutions and error norms are computed for each case using Eq. (18) and presented in Table 1. The control net, elements, boundary collocation points and associated boundary control points are presented in Fig. 4 for the case of grid 2. For this case, contour plot of the field variable is shown in Fig. 5. To save space, only one case is shown here in Figs. 4 and 5 and the other results are presented in Table 1. The convergence plot of the error norms are also shown in Fig. 6 for the proposed method and direct method of imposition of essential boundary conditions. As it can be seen from this figure, the error norms obtained from the proposed method are considerably less than the direct method. It is also clear that the error norms decrease by reducing the grid size.

Table 1. Error norms for example 1

	NCP	h	e (Direct)	e (present)	e (FEM)
Grid 1	9	5.00E-01	5.84E-01	1.96E-01	6.69E-01
Grid 2	16	3.33E-01	1.63E-01	5.23E-02	2.39E-01
Grid 3	25	2.50E-01	8.79E-02	3.27E-02	1.14E-01
Grid 4	36	2.00E-01	5.05E-02	1.76E-02	6.41E-02
Grid 5	49	1.67E-01	3.34E-02	1.17E-02	3.99E-02
Grid 6	64	1.43E-01	2.35E-02	7.90E-03	2.68E-02
Grid 7	81	1.25E-01	1.75E-02	5.69E-03	1.89E-02
Grid 8	121	1.00E-01	1.07E-02	3.26E-03	1.06E-02
Grid 9	169	8.33E-02	7.24E-03	2.07E-03	6.59E-03
Grid 10	225	7.14E-02	5.21E-03	1.41E-03	4.43E-03
Grid 11	289	6.25E-02	3.92E-03	1.01E-03	3.13E-03

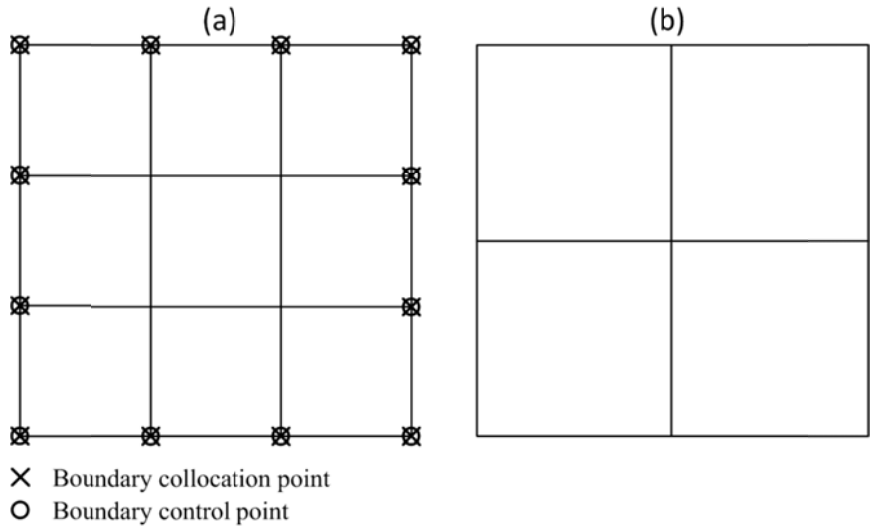

Fig. 4. Computational grid (grid 2) used in the solution of example 1, (a) Control net, (b) Elements

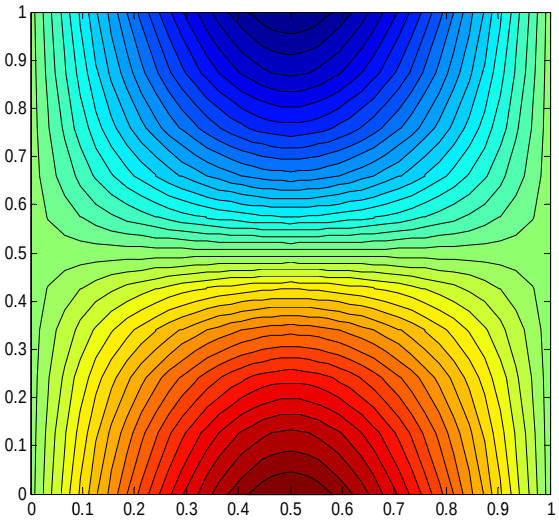

Fig. 5. Contour plot of the field variable in example 1, for the case of grid 2

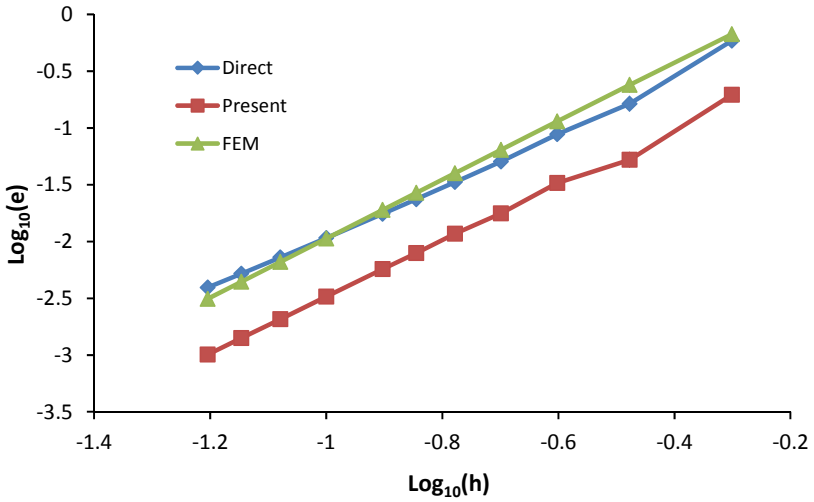

Fig. 6. Error norm of example 1, for different discretization levels obtained using direct method, proposed method and finite element

Example 2: Heat conduction in an annulus

As another potential problem, consider an annular region where its dimensions are shown in Fig. 7. The following source function is defined over the entire domain.

$$S = 6x + 12y^2 \tag{22}$$

The essential boundary conditions on the inner and outer boundaries are computed according to the following solution field.

$$u = x^3 + y^4 \tag{23}$$

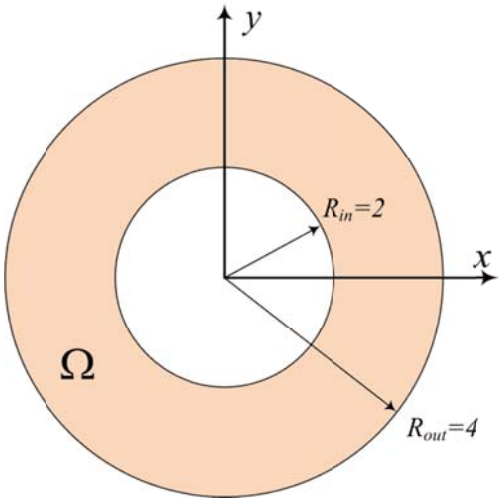

Fig. 7. Annular domain, example 2

The NURBS basis functions with suitable weights can reproduce circular arcs; therefore, the annular geometry of the present problem can also be described by NURBS basis functions exactly.

Similar to the previous example, for evaluating the convergence of the proposed method, the problem is solved using 4 different cases of control nets. The error norms are computed for each case using Eq. (18) and presented in Table 2. The control net, elements, boundary collocation points and associated boundary control points are presented in Fig. 8 only for the case of grid 1. Contour plot of the field variable is also shown in Fig. 9 for this case. The convergence plot of the error norms are shown in Fig. 10 for the proposed method and direct method of imposition of essential boundary conditions. Similar to

example 1, the error norms which are obtained from the proposed method considerably less than the direct method. It is also clear that the error norms decrease by reducing the grid size. It must be noted that in the present example, unlike the prior example, the boundary control points do not lay on the physical problem boundary.

Table 2. Error norms for example 2

	NCP	h	e (Direct)	e (Present)	e (FEM)
Grid 1	24	2.36E+00	2.19E-01	1.71E-01	7.08E-01
Grid 2	64	1.18E+00	8.88E-02	4.27E-02	1.41E-01
Grid 3	192	5.89E-01	2.63E-02	6.63E-03	3.31E-02
Grid 4	620	3.04E-01	7.06E-03	1.41E-03	8.89E-03

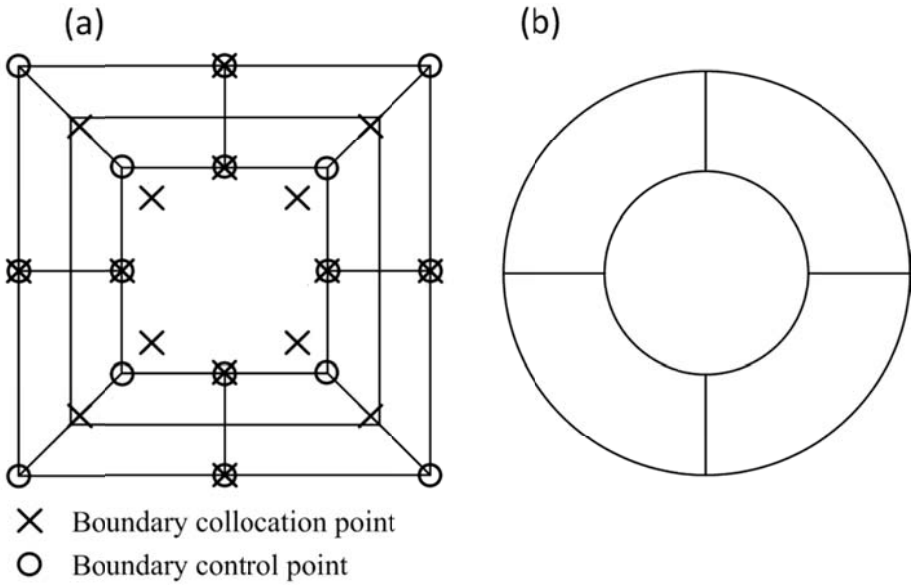

Fig. 8. Computational grid (grid 1) used in the solution of example 2, (a) Control net, (b) Elements

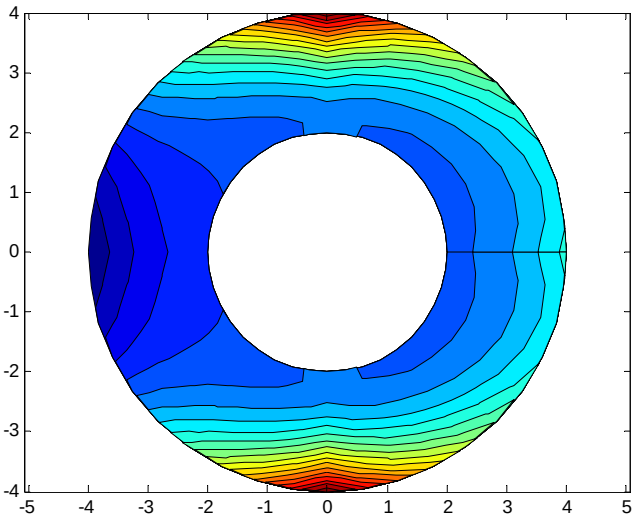

Fig. 9. Contour plot of the field variable in example 2, for the case of grid 1

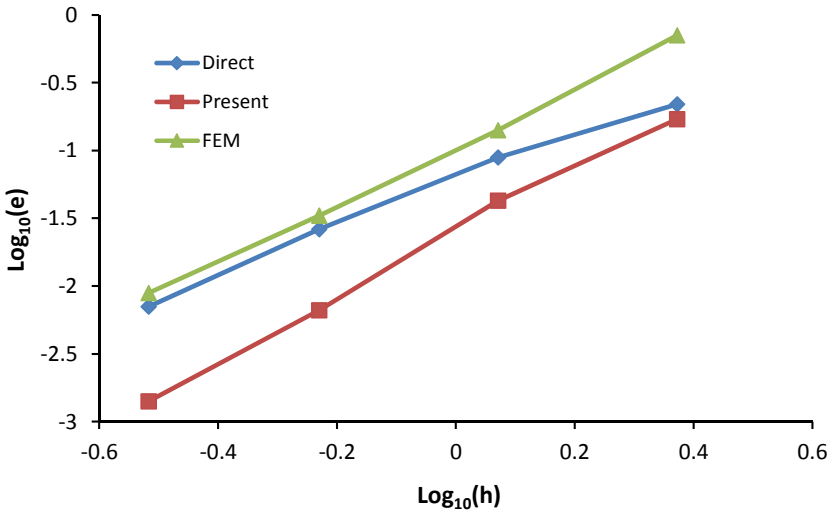

Fig. 10. Error norm of example 2, for different discretization levels obtained using direct method, proposed method and finite element

Example 3: Elastostatic of a cantilever beam

In this example a cantilever beam under a distributed end loading is considered. A schematic representation of this problem and its boundary conditions are shown in Fig. 11. The beam dimensions are as $D = 1\,m$ and $L = 3\,m$.The material is considered as linear elastic with $E = 200\,GPa$ and $\nu = 0.26$. The exact displacement and stress fields can be obtained using theory of elasticity [17] as follows.

$$u = \frac{P}{6EI}\left(3x^2y - 6Lxy + \frac{2+\nu}{4}D^2y - (2+\nu)y^3\right)$$
$$v = \frac{P}{6EI}\left(-x^3 + 3Lx^2 + \frac{4+5\nu}{4}D^2x - 3\nu xy^2 + 3Lvy^2\right) \quad (24)$$
$$\sigma_{xx} = \frac{P}{I}(-xy + Ly), \quad \sigma_{yy} = 0, \quad \sigma_{xy} = \frac{P}{2I}\left(\frac{D^2}{4} - y^2\right)$$

In these relations, $I = D^3/12$ is the moment of inertia of the beam cross section.

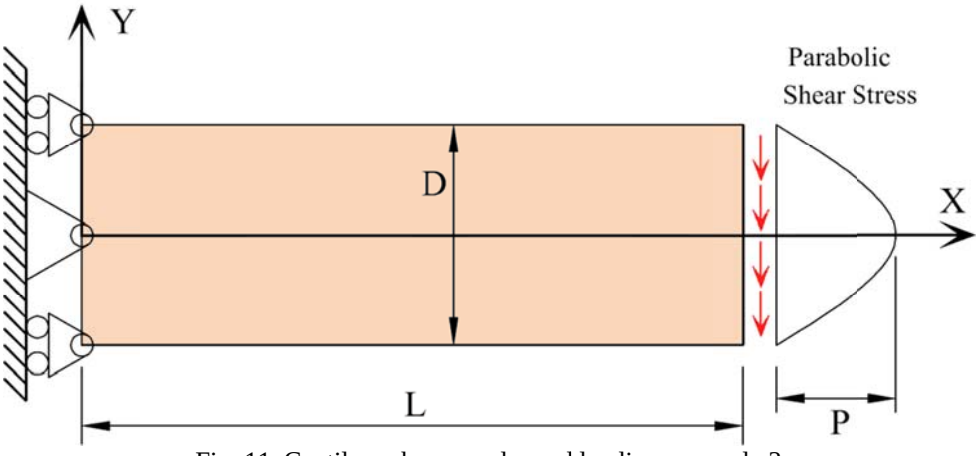

Fig. 11. Cantilever beam under end loading, example 3

The problem was solved with the proposed method using 3 different cases of control net. The relative error norm in displacement is computed using Eq. (19) and presented in Table 3. The error norms are also plotted in Fig. 12 for direct method, proposed method and standard finite element. It can be seen that the results for different grid types are in agreement with analytic solutions. It is also clear that the error norms which are obtained from the proposed method are considerably less than the direct method.

Table 3. Error norms for example 3

	NCP	h	e (Direct)	e (Present)	e (FEM)
Grid 1	9	2.50E-01	9.24E-04	2.51E-04	2.34E-03
Grid 2	16	1.25E-01	4.94E-05	1.97E-05	8.40E-05
Grid 3	25	6.25E-02	9.90E-07	3.94E-07	2.49E-06

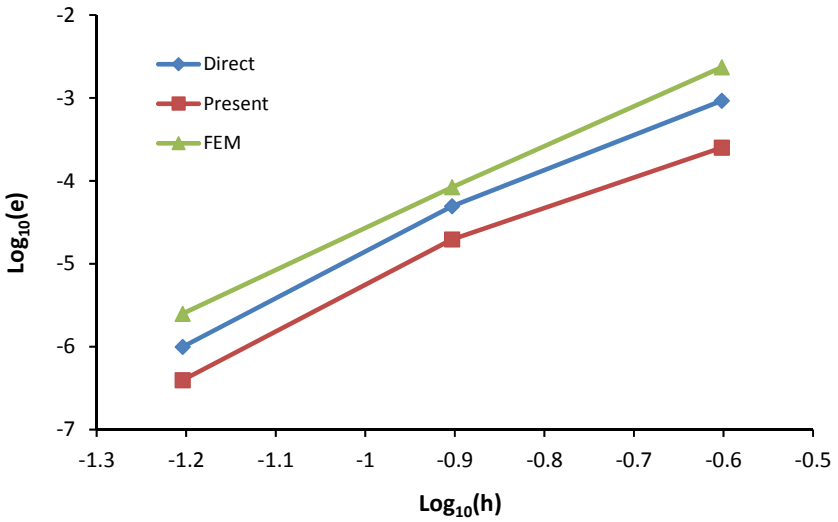

Fig. 12. Error norm of example 3, for different discretization levels obtained using direct method, proposed method and finite element

Example 4: Elastostatic of a thick walled cylinder

In the last example a thick walled cylinder with internal pressure is considered. Upon the symmetry of the problem only a quarter of the problem domain is considered and proper boundary conditions are applied on the cutting planes. A schematic diagram of the problem and boundary conditions is presented in Fig. 13. The problem has an analytical solution in the polar coordinates. The displacement and stress components in the Cartesian coordinates can be written as [17]

$$\begin{aligned} u &= \frac{Pa^2}{b^2-a^2}\frac{1+\nu}{E}\left((1-2\nu)r+\frac{b^2}{r}\right)\cos(\theta) \\ v &= \frac{Pa^2}{b^2-a^2}\frac{1+\nu}{E}\left((1-2\nu)r+\frac{b^2}{r}\right)\sin(\theta) \\ \sigma_{xx} &= \frac{Pa^2}{b^2-a^2}\left(1-\frac{b^2}{r^2}\cos(2\theta)\right) \\ \sigma_{yy} &= \frac{Pa^2}{b^2-a^2}\left(1+\frac{b^2}{r^2}\cos(2\theta)\right) \\ \sigma_{xy} &= -\frac{Pa^2b^2}{2(b^2-a^2)}\sin(2\theta) \end{aligned} \tag{25}$$

where, r and θ are measured in the polar coordinates. The material properties are $E = 200\ GPa$ and $\nu = 0.26$. The cylinder diameters are $a = 1\ m$ and b$= 2\ m$. The problem is solved with 3 control net resolution. The relative error norms in displacement obtained using different method is presented in Table 4 and shown in Fig. 14. The results show the proposed method is in good agreement with analytic solution and it is observed that the present method provides better results compared to the direct method.

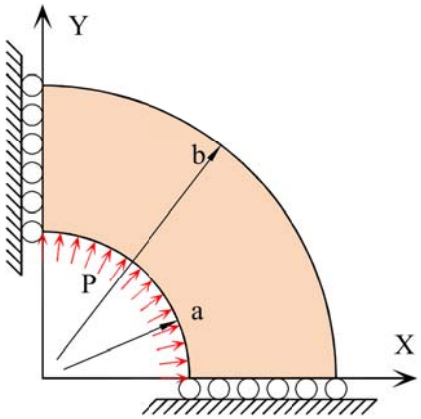

Fig. 13. Thick walled cylinder under internal pressure, example 4

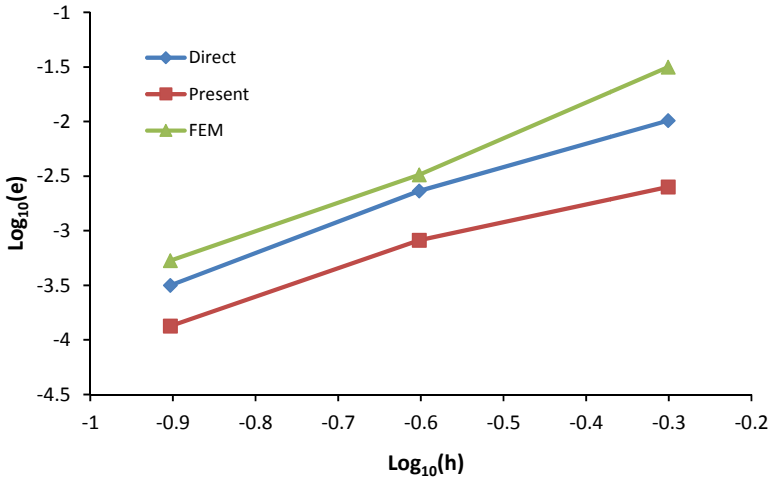

Fig. 14. Error norm of example 4, for different discretization levels obtained using direct method, proposed method and finite element

Table 4. Error norms for example 4

	NCP	h	e (Direct)	e (Present)	e (FEM)
Grid 1	16	5.00E-01	1.02E-02	2.51E-03	3.16E-02
Grid 2	25	2.50E-01	2.31E-03	8.19E-04	3.26E-03
Grid 3	36	1.25E-01	3.15E-04	1.34E-04	5.32E-04

7. CONCLUSION

Because of the non-interpolatory property of the NURBS basis functions, it is a challenging task to impose essential boundary conditions in the IA. In the present work, we have proposed a simple point collocation method for imposition of essential boundary conditions in the IA. In this method, the NURBS basis functions are used to derive a collocation equation for each distinct point on the essential boundary; these equations are then inserted into the global system of equations. To evaluate the performance of the proposed method, we considered two model boundary value problems and solved four numeric examples for different levels of discretization and also used the L_2 error norm in order to qualify the results. It was observed that the error level of the proposed method was significantly less than the direct method of imposition of boundary conditions on the control points. Therefore, it is believed that the proposed method can be effectively used in the imposition of essential boundary conditions in the isogeometric analysis of potential problems.

Acknowledgement- The results presented in this paper are from a research project supported by the Islamic Azad University, Shiraz Branch, Shiraz, Iran. Partial support of the first author by the Islamic Azad University, Shiraz Branch is also appreciated.

REFERENCES

1. Hughes, T. J. R., Cottrell, J. A. & Bazilevs, Y. (2005). Isogeometric analysis: CAD, finite elements, NURBS, exact geometry and mesh refinement. *Computer Methods in Applied Mechanics and Engineering*, Vol. 194, pp. 4135-4195.
2. Cottrell, J. A., Reali, A., Bazilevs, Y. & Hughes, T. J. R. (2006). Isogeometric analysis of structural vibrations. *Computer Methods in Applied Mechanics and Engineering*, Vol. 195, pp. 5257-5296.
3. Bazilevs, Y., Calo, V. M., Hughes, T. J. R. & Zhang, Y. (2008). Isogeometric fluid-structure interaction: theory, algorithms and computations. *Computational Mechanics*, Vol. 43, pp. 3-37.
4. Ha, S. H. & Cho, S. (2010). Numerical method for shape optimization using T-spline based isogeometric method. *Structural and Multidisciplinary Optimization*, Vol. 42, No. 3, pp. 417-428.
5. Bazilevs, Y., Michler, C., Calo, V. M. & Hughes, T. J. R. (2010). Isogeometric variational multi scale modeling of wall-bounded turbulent flows with weakly enforced boundary conditions on unstretched meshes. *Computer Methods in Applied Mechanics and Engineering*, Vol. 199, pp. 780-790.
6. Benson, D. J., Bazilevs, Y., Hsu, M. C. & Hughes, T. J. R. (2010). Isogeometric shell analysis: the Reissner-Mindlin shell. *Computer Methods in Applied Mechanics and Engineering*, Vol. 199, pp. 276-289.
7. Embar, A., Dolbow, J. & Harari, I. (2010). Imposing Dirichlet boundary conditions with Nitsche's method and spline-based finite elements. *International Journal for Numerical Methods in Engineering*, Vol. 83, pp. 877-898.
8. Bazilevs, Y. & Hughes, T. J. R. (2007). Weak imposition of Dirichlet boundary conditions in fluid mechanics. *Computers & Fluids*, Vol. 36, pp. 12-26.
9. Bazilevs, Y., Michler, C., Calo, V. M. & Hughes, T. J. R. (2007). Weak Dirichlet boundary conditions for wall-bounded turbulent flows. *Computer Methods in Applied Mechanics and Engineering*, Vol. 196, pp. 4853-4862.
10. Hinton, E. & Campbell, J. S. (1974). Local and global smoothing of discontinuous finite element functions using a least squares method. *International Journal for Numerical Methods in Engineering*, Vol. 8, pp. 461-480.
11. Mitchell, T. J., Govindjee, S. & Taylor, R. L. (2011). *A method for enforcement of dirichlet boundary conditions in isogeometric analysis*. in Mueller-Hoeppe, D., Loehnert, S., Reese, S., *Recent developments and innovative applications in computational mechanics*, Springer-Verlag, Berlin.
12. Chen, T., Mo, R. & Wan, N. (2011). NURBS based isogeometric finite element method for analysis of two-dimensional piezoelectric device. *Procedia Engineering*, Vol. 15, pp. 3562-3566.
13. Chen, T., Mo, R. & Gong, Z. (2012). Imposing essential boundary conditions in isogeometric analysis with Nitsche's method. *Applied Mechanics and Materials*, Vols. 121-126, pp. 2779-2783.
14. Wang, D. & Xuan, J. (2010). An improved NURBS-based isogeometric analysis with enhanced treatment of essential boundary conditions. *Computer Methods in Applied Mechanics and Engineering*, Vol. 199, pp. 2425-2436.
15. Piegl, L. & Tiller, W. (1997). *The NURBS Book: Monographs in visual communication*. Second Edition, Springer-Verlag, New York, 1997.
16. Reddy, J. N. (1993). *An introduction to the finite element method*. 2nd edition, McGraw-Hill.
17. Timoshinko, S. P. & Goodier, J. N. (1970). *Theory of elasticity*. Third edition, McGraw-Hill, New York.